MOLECULAR AND CELLULAR BIOLOGY, Aug. 2005, p. 6338–6345 Vol. 25, No. 15
0270-7306/05/$08.00+0 doi:10.1128/MCB.25.15.6338–6345.2005

ISG15, an Interferon-Stimulated Ubiquitin-Like Protein, Is Not Essential for STAT1 Signaling and Responses against Vesicular Stomatitis and Lymphocytic Choriomeningitis Virus

Anna Osiak,[1] Olaf Utermöhlen,[3] Sandra Niendorf,[1] Ivan Horak,[1,2] and Klaus-Peter Knobeloch[1]*

Abteilung für Molekulare Genetik, Institut für Molekulare Pharmakologie,[1] and Charité Universitätsmedizin,[2] Berlin, Germany, and Institut für Medizinische Mikrobiologie, Immunologie und Hygiene, Universität Köln, Köln, Germany[3]

Received 20 December 2004/Returned for modification 7 March 2005/Accepted 1 May 2005

ISG15 is an interferon-induced ubiquitin-like modifier which can be conjugated to distinct, but largely unknown, proteins. ISG15 has been implicated in a variety of biological activities, which encompass antiviral defense, immune responses, and pregnancy. Mice lacking UBP43 (USP18), the ISG15-deconjugating enzyme, develop a severe phenotype with brain injuries and lethal hypersensitivity to poly(I:C). It has been reported that an augmented conjugation of ISG15 in the absence of UBP43 induces prolonged STAT1 phosphorylation and that the ISG15 conjugation plays an important role in the regulation of JAK/STAT and interferon signaling (O. A. Malakhova, M. Yan, M. P. Malakhov, Y. Yuan, K. J. Ritchie, K. I. Kim, L. F. Peterson, K. Shuai, and D. E. Zhang, Genes Dev. 17:455–460, 2003). Here, we report that ISG15$^{-/-}$ mice are viable and fertile and display no obvious abnormalities. Lack of ISG15 did not affect the development and composition of the main cellular compartments of the immune system. The interferon-induced antiviral state and immune responses directed against vesicular stomatitis virus and lymphocytic choriomeningitis virus were not significantly altered in the absence of ISG15. Furthermore, interferon- or endotoxin-induced STAT1 tyrosine-phosphorylation, as well as expression of typical STAT1 target genes, remained unaffected by the lack of ISG15. Thus, ISG15 is dispensable for STAT1 and interferon signaling.

Interferons (IFNs) are cytokines that communicate signals for a broad spectrum of cellular activities that encompass antiviral and immunomodulatory responses, as well as growth regulation. These pleiotropic cellular activities are mediated through a large number of proteins whose expression is triggered by activated interferon receptors present on almost all cells (3, 32). Intensive research established JAK/STAT as the principal intracellular signaling pathway downstream of interferon receptors (9, 15, 25). Despite great progress, our understanding of the complex IFN activities remains incomplete.

Interferon-stimulated gene 15/ubiquitin cross-reacting protein (designated ISG15/UCRP) is a 15-kDa ubiquitin-like protein identified as a product of an IFN-stimulated gene in humans (11). ISG15-homologous genes were found in several other species but are absent in yeast (26). ISG15 expression is induced in many cell types by IFNs, viral infection, bacterial endotoxins, double-stranded RNA, and genotoxic stress (7). Congruently, transcription factors of the interferon regulatory factor family (IRF) (IRF-1, IRF-3, IRF-4, IRF-7, and ICSBP/IRF-8) that bind to the interferon-stimulated response element motif in the regulatory DNA region of ISG15, together with the *ets* factor PU.1, regulate ISG15 expression (28). ISG15 was also found to be strongly induced by NEMO/IκB signaling (16).

The mature ISG15 polypeptide is generated from a precursor by specific cleavage of the carboxyl-terminal extension (26), a feature common to several ubiquitin-like proteins. The ISG15 protein consists of two ubiquitin-like domains with an overall sequence similarity to ubiquitin of 59.3%. Moreover, the fold-determining sequences of ubiquitin are also very highly conserved in ISG15 (7). ISG15 contains the canonical LRGG motif at its C terminus, which is required for conjugation of ubiquitin and ubiquitin-like proteins to their targets. Similar to conjugation of ubiquitin and other ubiquitin-like molecules, such as SUMO or NEDD8, ISG15 is ligated by an isopeptide bond to several target proteins (17). UBE1L and UbcH8 were identified as E1- and E2-conjugating enzymes for ISG15, respectively (34, 35). Recently, as a first protein substrate to which ISG15 is conjugated, serine-protease inhibitor (serpin 2a) was identified by mass spectrometry (8).

The functional significance of the protein modification by ISG15 conjugation (ISGylation) is not yet known. However, the following observations strongly suggested that it may have important physiological activity. Conjugation of ISG15 to several cellular proteins increases rapidly after endotoxin (lipopolysaccharide [LPS]) and interferon induction (7, 21). In parallel with accumulating evidence for interference of viruses with the ubiquitination/deubiquitination machinery of the cell (31), the NS1 protein of the human influenza B virus inhibits ISGylation (34).

* Corresponding author. Mailing address: Institute of Molecular Pharmacology, Department of Molecular Genetics, Krahmerstr. 6, 12207 Berlin, Germany. Phone: 49 3084371915. Fax: 49 3084371922. E-mail: knobeloch@fmp-berlin.de.

It has been reported that ISG15 is secreted by human monocytes and lymphocytes, displaying the properties of an interferon-induced cytokine (5). According to these authors, ISG15 induces IFN-γ production by T cells, stimulates the T-cell-dependent expansion of natural killer cells ($CD56^+$), and augments non-major histocompatibility class (MHC)-restricted cytolytic activity against tumor cell targets. However, these observations have not been extended further, so the molecular basis and the biological significance remain uncertain.

Another role may be ascribed to ISG15 during pregnancy. ISG15 expression in endometrium during pregnancy has been reported for several species, including the mouse (2).

Recently, UBP43 (USP18), a specific protease which removes protein-conjugated ISG15, was identified (19). UBP43-deficient mice have elevated levels of ISG15 conjugates, develop brain injury due to necrosis of ependymal cells, and die early (27). Using immunoprecipitations and high-throughput Western blotting, several key regulators of signal transduction (JAK1, STAT1, ERK1, and phospholipase Cγ1) were found to be modified by ISG15 conjugation (18). The same group reported that in the absence of UBP43, IFN-β induced an extensive activation of JAK/STAT signaling, marked by a prolonged STAT1 phosphorylation and IFN-mediated gene activation. They concluded that ISG15 modification plays an important role in the regulation of interferon signaling (20, 28).

The speculations on biological activities of free and conjugated ISG15 are further nourished by the increasing recognition of diverse functions of ubiquitin and ubiquitin-related protein modification (30). Since direct and rigorous evidence for a physiological role of ISG15 has not yet been provided, we generated ISG15-deficient mice by gene targeting and analyzed the consequences of the lack of ISG15 and ISG15 protein modification in vivo.

MATERIALS AND METHODS

Generation of ISG15-deficient mice and genotyping. For the generation of $ISG15^{-/-}$ mice, the genomic DNA of the ISG15 gene was isolated from a 129/Sv PAC mouse genomic library (Resource Center of the German Human Genome Project, MPI for Molecular Genetics, Berlin, Germany). A targeting vector was constructed from a 4-kb PCR fragment containing the 5′ end and exon I (including translation-initiation codon ATG) of the ISG15 gene and a 2.5-kb SpeI fragment containing the 3′ region of the ISG15 gene. The second exon of the ISG15 gene, including the open reading frame apart from the first ATG, was replaced by a *neo* cassette flanked by two *loxP* sites (Fig. 1). Embryonic stem (ES) cells were electroporated with a KpnI-linearized target vector and grown under double selection as previously described (10). Seven ES cell clones carrying the desired mutation were identified by the presence of an additional 2.8-kB BamHI fragment detected by a 3′ probe (Fig. 1). Two independent clones were used for injection into C57BL/6 blastocysts to generate germ line chimeras. ISG15-deficient animals were generated by interbreeding of heterozygous offspring. Mice were genotyped with the following primers: 5′-GCCCCCATCCAGAGCCAGT GTT-3′ and 5′-AGCCCCGATGAGGATGAGGTGT-3′ for the wild-type ISG15 allele and 5′-CGCGAAGGGGCCACCAAAGAA-3′ and 5′-AGCCCCGATGA GGATGAGGTGT-3′ for the mutated ISG15 allele. Mice used for analysis were on a 129OLA–C57BL/6 mixed background if not mentioned otherwise. For analyses of NK cells, mice backcrossed to C57BL/6 over six generations were used.

Generation of anti-ISG15 antisera. The part of the murine ISG15 cDNA, encoding the open reading frame of the mature protein (Ala^2 to Gly^{153}), was amplified using primers 5′-GACCGCGGTCTCGGCGCCGCCTGGGACCTA AAGGTGAAGATGC-3′ and 5′-GCTAATTAAGCTTACCCACCCCTCAGG CGCAAATGC-3′. The amplification product was subsequently digested with BsaI and HindIII endonucleases and cloned into pASK-IBA5 vector (IBA, Göttingen, Germany). The resulting bacterial expression vector was transfected in *Escherichia coli*; upon lysis, recombinant ISG15 protein fused to the N-terminal StrepII affinity tag was purified via Strep-tactin columns according to the manufacturer's protocol. Recombinant protein was dialyzed against phos-

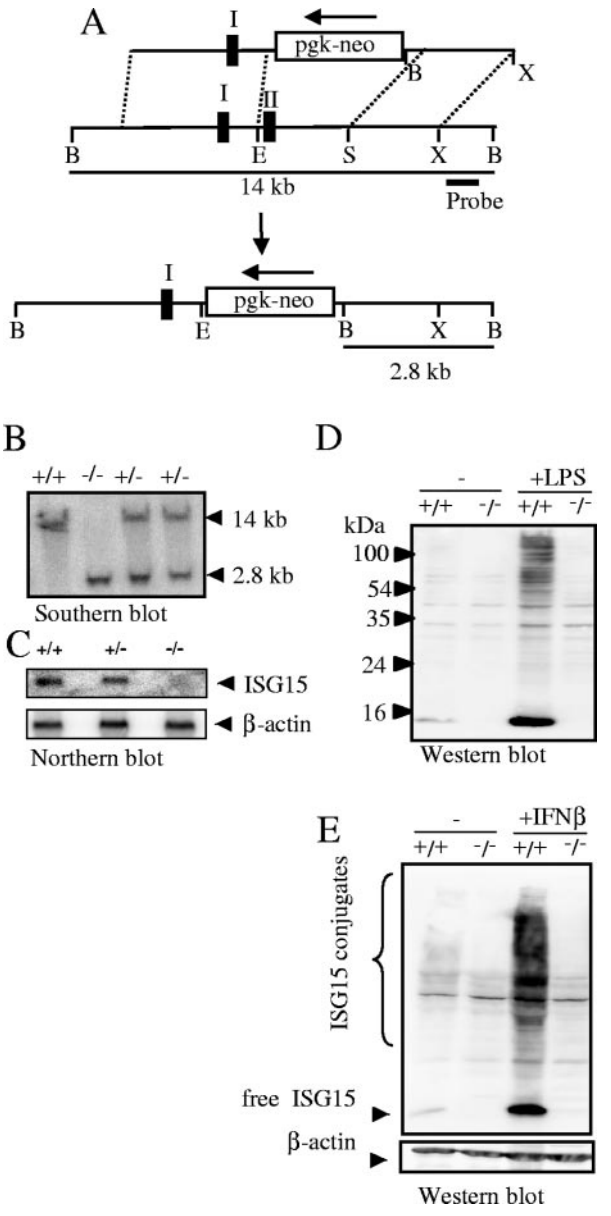

FIG. 1. ISG15 gene inactivation. (A) Knockout strategy. Restriction maps are shown for the targeting vector (top), wild-type ISG15 gene locus (middle), and mutated ISG15 gene locus after homologous recombination (bottom). Exons are indicated as black boxes. The orientation of the neomycin (neo) resistance marker under control of the phosphoglycerate kinase promoter (pgk) is shown by an arrow. The target vector was linearized by KpnI. Restriction sites: B, BamHI; E, EcoRI; S, SpeI;X, XhoI. (B) Southern blot analysis of littermates from $ISG15^{+/-}$ matings. A 219-bp PCR-fragment adjacent to the 3′ homology was used as a probe and detected a 14-kb or 2.8-kb BamHI fragment characteristic for the wild type or the mutant allele, respectively. (C) Lack of ISG15 mRNA in $ISG15^{-/-}$ mice. Bone marrow cells were stimulated with IFN-β for 16 h and analyzed by Northern blot hybridization using full-length ISG15 cDNA as a probe. Upon stripping, a β-actin-specific probe was hybridized to the filter as a loading control. (D and E). Lack of free ISG15 protein and ISG15 conjugation in $ISG15^{-/-}$ mice. BMM from $ISG15^{+/+}$ and $ISG15^{-/-}$ mice were treated with 100 ng/ml LPS (D) or 1,000 U IFN (E) for 24 h and analyzed by Western blotting with anti-ISG15 antibody.

TABLE 1. Frequency of cell populations in lymphoid organs of ISG15$^{+/+}$ and ISG15$^{-/-}$ mice

Tissue type	Cell type	Surface marker	% Cells[a]	
			ISG15$^{+/+}$	ISG15$^{-/-}$
Thymus	Double-positive thymocytes	CD4$^+$ CD8$^+$	71.7 ± 1.9	76.7 ± 1.4
	CD4$^+$ thymocytes	CD4$^+$ CD8$^-$	14.4 ± 0.8	12.3 ± 0.8
	CD8$^+$ thymocytes	CD4$^-$ CD8$^+$	4.6 ± 0.3	4.1 ± 0.4
	Double-negative thymocytes	CD4$^-$ CD8$^-$	9.4 ± 1.2	6.9 ± 0.9
Bone marrow	Blast cells (progenitor and stem cells)	CD31^{high} Ly6-C^{low}	2.4 ± 0.1	2.4 ± 0.1
	Lymphoid cells	CD31^{intermediate} Ly6-C^{low}	14.1 ± 0.6	14.9 ± 0.5
	Erythroid progenitor cells	CD31^{low} Ly6-C^{low}	4.0 ± 0.5	4.6 ± 0.2
	Myeloid progenitor cells	CD31^{positive} Ly6-C^{positive}	13.6 ± 0.3	13.8 ± 0.3
	Granulocytes	CD31^{low} Ly6-C^{intermediate}	40.9 ± 0.8	40.7 ± 0.6
	Monocytes	CD31^{low} Ly6-C^{high}	18.9 ± 1.3	17.4 ± 0.5
Spleen	CD4$^+$ T cells	CD3$^+$ CD4$^+$	14.7 ± 0.6	15.0 ± 0.7
	CD8$^+$ T cells	CD3$^+$ CD8$^+$	10.3 ± 0.6	13.9 ± 1.0
	Immature B cells	B220$^+$ IgM^{high} IgD^{low}	13.1 ± 0.8	14.7 ± 0.5
	Mature B cells	B220$^+$ IgM^{low} IgD^{high}	33.7 ± 2.8	27.2 ± 3.9
	Granulocytes	Gr1^{high} F4/80^{low}	1.2 ± 0.3	1.4 ± 0.4
	Monocytes	CD11b^{low} F4/80^{low}	4.4 ± 0.2	5.8 ± 0.5
	Eosinophils	CD11b$^-$ F4/80^{intermediate}	2.6 ± 0.2	3.3 ± 0.2
Lymph node	CD4$^+$ T cells	CD3$^+$ CD4$^+$	33.1 ± 1.3	38.6 ± 1.1
	CD8$^+$ T cells	CD3$^+$ CD8$^+$	32.4 ± 1.4	32.2 ± 1.6
	B cells	B220$^+$ IgM$^+$	19.0 ± 1.6	17.2 ± 1.7
	Granulocytes	Gr1^{high} F4/80^{low}	0.1 ± 0.0	0.1 ± 0.0
	Monocytes	CD11b^{low} F4/80^{low}	1.5 ± 0.3	1.1 ± 0.3
	Eosinophils	CD11b$^-$ F4/80^{intermediate}	0.3 ± 0.0	0.3 ± 0.0

[a] Mean percentage ± SEM is given for groups of 5 to 12 animals analyzed in two or more independent experiments.

phate-buffered saline (PBS) and used to immunize rabbits. The resulting antisera were affinity purified using glutathione *S*-transferase–ISG15 recombinant protein expressed in *E. coli*.

Cytokines, reagents, and antibodies. poly(I:C), IFN-α/β, IFN-γ, and LPS from *E. coli* O55:B5 were purchased from Sigma. STAT1 mouse monoclonal antibody (MAb) and STATp Tyr701 (rabbit) antibody were from Cell Signaling; anti-actin (goat) antisera were from Santa Cruz.

Western blotting. Cells in 6-cm dishes were treated as indicated in the figure legends and lysed at different time points with radioimmunoprecipitation assay buffer containing protease inhibitors (Boehringer). Protein was loaded on sodium dodecyl sulfate-containing polyacrylamide gels; upon separation, it was blotted to nitrocellulose by standard techniques. Western blots were incubated with primary antibodies according to the manufacturer's protocol, and secondary antibodies were coupled to horseradish peroxidase. Blots were then developed using ECL reagent (Amersham).

TABLE 2. Frequency of cell populations after 3 days of in vivo stimulation with daily injections of 0.5 mg poly(I:C)

Tissue type	Phenotype	% of mice with lymphocyte phenotype[a]	
		ISG15$^{+/+}$	ISG15$^{-/-}$
Thymus	CD4$^+$ CD8$^+$	70.3 ± 1.5	72.6 ± 1.9
	CD4$^+$ CD8$^-$	18.8 ± 1.1	18.9 ± 1.1
	CD4$^-$ CD8$^+$	4.3 ± 0.4	3.8 ± 0.5
	CD4$^-$ CD8$^-$	5.8 ± 1.3	4.5 ± 0.6
Spleen	CD3$^+$ CD4$^+$	17.2 ± 1.4	15.6 ± 0.5
	CD3$^+$ CD8$^+$	8.3 ± 0.5	7.7 ± 0.5
	B220$^+$ IgM^{high} IgD^{low}	50.6 ± 1.9	47.9 ± 1.7
	B220$^+$ IgM^{low} IgD^{high}	1.7 ± 0.2	1.9 ± 0.1
	Gr1^{high} F4/80^{low}	2.6 ± 0.1	2.7 ± 0.3
	CD11b^{low} F4/80^{low}	2.6 ± 0.2	3.2 ± 0.5
	CD11b$^-$ F4/80^{intermediate}	0.2 ± 0.0	0.2 ± 0.0

[a] Mean percentage ± standard error of the mean is given for groups of 5 to 12 animals analyzed in two or more independent experiments.

Antibodies and flow cytometry. Single-cell suspensions were prepared from the thymuses, spleens, bone marrow, and lymph nodes of 6- to 8-week-old mice. All cells were subjected to hypotonic lysis of red blood cells by 12 min of incubation in a solution containing 150 mM NH_4Cl, 15 mM Na_2CO_3, and 0.1 mM EDTA (pH 7.3), followed by washing in PBS containing 2% newborn calf serum, 0.1% NaN_3, and 2 mM EDTA and staining with antibodies against cell surface molecules. For flow cytometric analysis, the unlabeled, biotinylated, phycoerythrin-, allophycocyanin-, or fluorescein isothiocyanate-conjugated antibodies against the following cell surface molecules were used: CD3ε (145-2C11), CD4 (RM4-5), CD8α (53-6.7), CD11b (M1/70), Gr1 (RB6-8C5), CD45R/B220 (RA3-6B2), immunoglobulin D (IgD) (11-26c.2a), IgM (R6-60.2), I-A^b (25-9-17), H2K^b (AF6-88.5), pan-NK (DX5), NK1.1 (NKR-P1C), Ly6C (AL-21), and CD31 (MEC 13.3) (all from PharMingen) and F4/80 (Serotec). Biotinylated antibodies were visualized with fluorescein isothiocyanate-, or allophycocyanin-, or phycoerythrin-conjugated streptavidin (PharMingen). Samples were analyzed on a FACSCalibur flow cytometer (Becton Dickinson) according to standard protocols. Gates on viable cells were set according to the exclusion of propidium iodide staining. To measure the frequency of virus-specific CD8$^+$ cytotoxic T lymphocytes, phycoerythrin-labeled H-2D^b tetramers loaded with one of the three H-2D^b-restricted epitopes ($NP_{396–404}$, $GP_{33–41}$, or $GP_{276–286}$) were used in conjunction with fluorescein isothiocyanate-labeled CD8-specific MAb (KT15) according to the instructions of the manufacturer (ProImmune).

TABLE 3. Frequency of NK cells in spleens of ISG15-deficient mice[a]

Duration of poly(I:C) treatment and dose	Phenotype	% of total cells in spleen	
		ISG15$^{+/+}$	ISG15$^{-/-}$
36 h			
0 μg	CD3$^-$ DX5$^+$	8.4 ± 0.3	8.1 ± 0.7
500 μg	CD3$^-$ DX5$^+$	13.2 ± 1.2	12.6 ± 0.7
3 days			
500 μg/day	CD3$^-$ DX5$^+$	20.3 ± 1.3	21.1 ± 0.9

[a] Mean percentage ± standard error of the mean is given for groups of 5 to 12 animals analyzed.

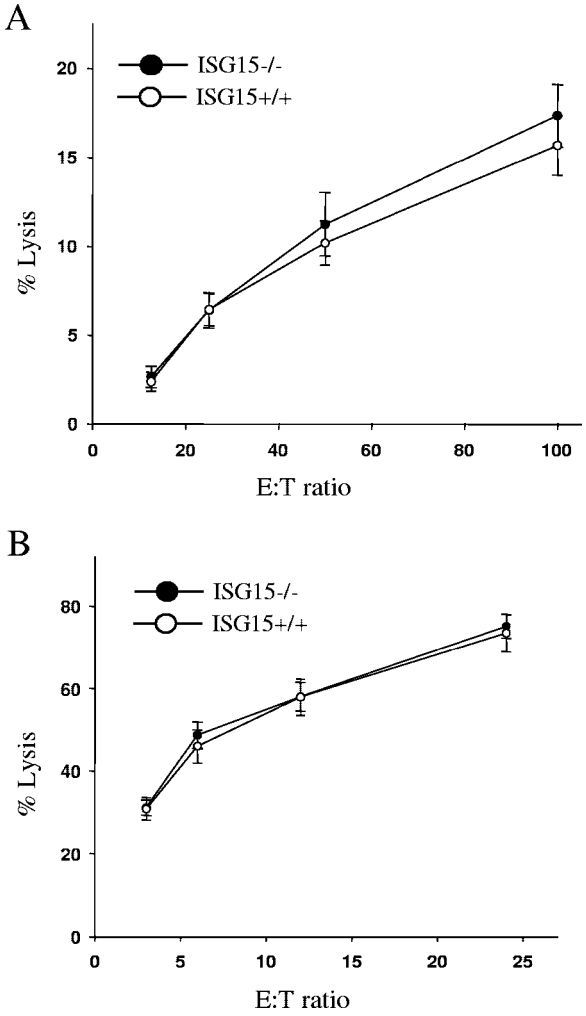

FIG. 2. Cytolytic activity of ISG15$^{-/-}$ NK cells. (A) Unfractionated splenocytes isolated from poly(I:C)-treated mice were incubated for 4 h with ^{51}Cr-labeled NK-sensitive YAC-1 target cells at the indicated effector-to-target ratios. Results are the means ± standard error of the mean (SEM) of six mice in each group. (B) NK cells from splenocytes of ISG15$^{-/-}$ and ISG15 $^{+/+}$ mice were enriched by positive magnetic cell sorting against DX5 and incubated for 4 h with ^{51}Cr-labeled NK-sensitive YAC-1 target cells at the indicated effector-to-target ratios. Results are the means ± SEM of six mice in each group.

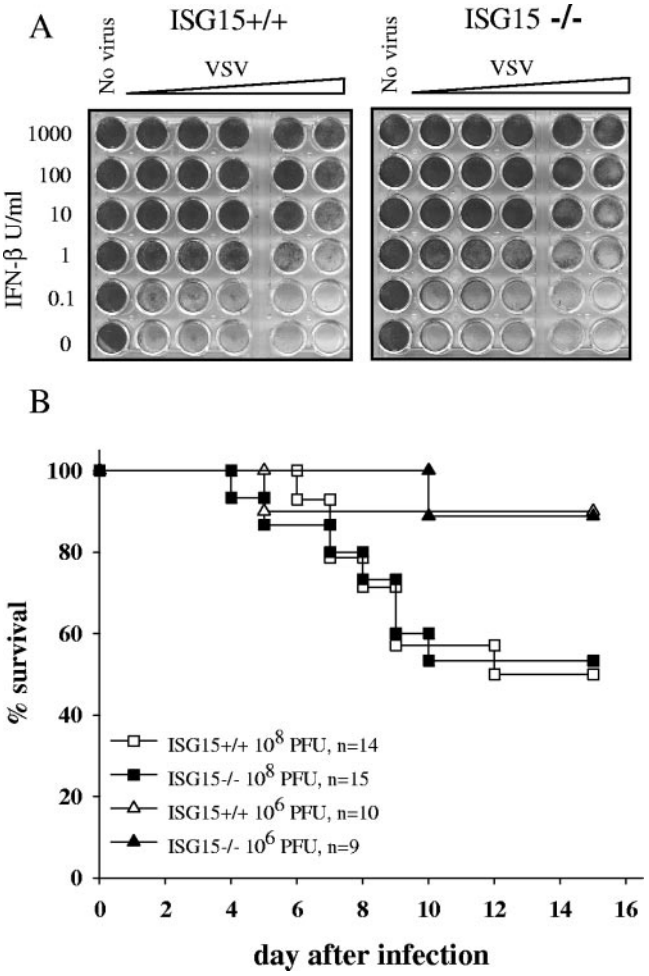

FIG. 3. Antiviral response of ISG15$^{-/-}$ cells and survival of ISG15$^{-/-}$ mice upon VSV infection. (A) Wild-type and ISG15$^{-/-}$ embryonic fibroblasts were incubated with serial dilutions of recombinant murine IFN-β as indicated. After 24 h, cell cultures were challenged with VSV, and cell viability was monitored 24 h later by vital dye uptake. (B) Wild-type and ISG15$^{-/-}$ mice were infected i.v. with 10^8 or 10^6 PFU VSV and monitored daily for survival.

Frequency of NK cells after stimulation with poly(I:C). Mice used in this experiment were backcrossed to the C57/B6 genetic background for at least 6 generations. Mice (6 to 8 weeks old) were injected intraperitoneally with 0.5 mg poly(I:C) in 0.5 ml PBS. Control mice were treated with 0.5 ml PBS. Animals were killed after 36 h, and single-cell suspensions were prepared from their spleens. Alternatively, a daily injection of 0.5 mg/ml poly(I:C) for 3 days was administered. After hypotonic lysis of red blood cells, the cell suspensions were stained with antibodies against CD3ε (145-2C11) and pan-NK (DX5) (PharMingen). Samples were analyzed on a FACSCalibur flow cytometer (Becton Dickinson) according to standard protocols.

Cytotoxicity assay. Cytotoxic activity of NK cells was assessed against ^{51}Cr-labeled YAC-1 target cells by a standard ^{51}Cr release assay. Effector cells consisted of splenocytes that had been stimulated in vivo for 24 h by intraperitoneal injection of 100 μg poly(I:C)/mice (Sigma). Alternatively as effector cells, NK cells were used that had been enriched by positive selection from splenocytes using anti-DX5 paramagnetic beads according to the manufacturer's protocol (Miltenyi Biotech). This procedure typically yielded a cell population consisting of 70 to 80% DX5$^+$ cells. YAC-1 target cells were labeled with 100 μCi sodium (^{51}Cr-labeled) chromate for 2 h at 37°C. Labeled target cells were washed three times and plated at 10^4 cells per well with appropriately diluted effector cells. After 4 h, supernatants were counted with a scintillation counter. The percent specific lysis was calculated as [(experimental release − spontaneous release)/(maximum release − spontaneous release)] × 100.

Cell culture. Bone marrow-derived macrophages (BMM) were generated as previously described (29). Briefly, bone marrow from mice was isolated and subjected to erythrocyte lysis. Remaining cells were plated in non-tissue-culture plates in media containing 25% L-cell-conditioned medium as a source of interleukin-3. After 7 days, the resulting bone marrow macrophages were harvested and used for further experiments. Murine embryonic fibroblasts (MEFs) were derived by disaggregation of day 13.5 embryos from timed matings by stirring the embryos at 37°C in trypsin with glass beads. Cells were used up to a maximum passage number of six.

Antiviral activity assay. The ability of MEFs to resist vesicular stomatitis virus (VSV) infection was determined using a cytopathic effect assay (13, 14). Briefly, MEF cells were seeded into 24-well plates at a density of 10^5 per well and incubated with serial dilutions of recombinant murine IFN-β (Calbiochem) as indicated. After 24 h, cells were incubated with different doses of VSV (Indiana strain) ranging from 10^4 PFU/well to 10^8 PFU/well. At 24 h after infection, cell viability was determined by crystal violet staining.

Viral infections. The Indiana strain of VSV, kindly provided by Ulrich Kalinke, was propagated and titrated on BHK cells. Mice were injected intravenously (i.v.) with doses of either 10^8 or 10^6 PFU in 0.3 ml PBS and monitored

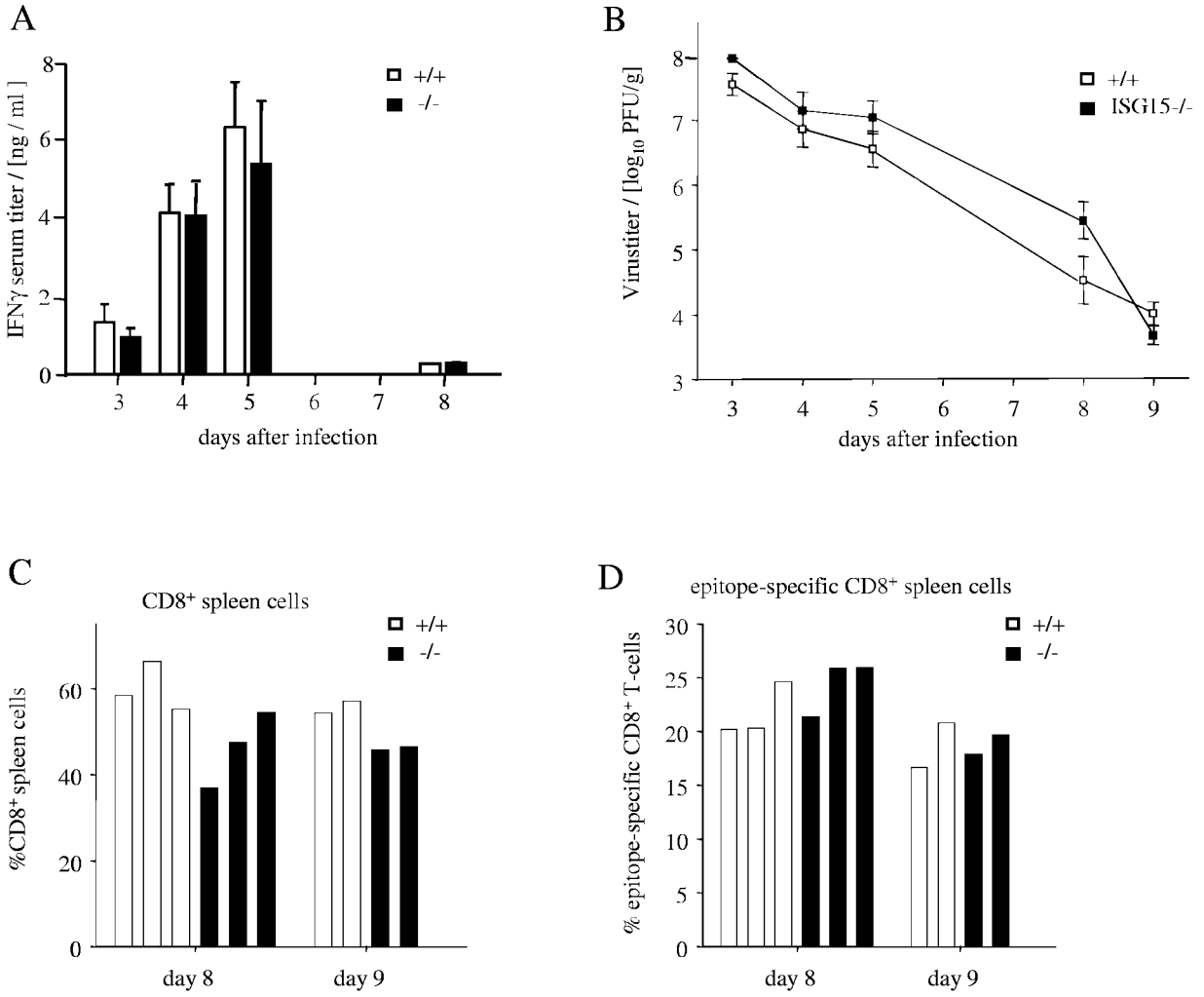

FIG. 4. Immune response during acute infection of wild type and ISG15$^{-/-}$ mice with LCMV. (A) IFN-γ in sera of mice during the course of LCMV infection. Mice were infected i.v. with 10^5 IU of LCMV and bled on the indicated days. IFN-γ was determined by an enzyme-linked immunosorbent assay. Shown are the means of levels from two mice per group on days 3, 5, and 8, and the mean and SEM for three mice on day 4. (B) Elimination of the LCMV from the spleens of acutely infected mice. Mice were infected i.v. with 10^5 IU of LCMV. On the indicated days, the virus titer in the spleen was determined as the number of PFU per gram of spleen. Shown are the mean and standard error for groups of the following sizes: day 3, two mice; day 4, nine mice; day 5, two mice; day 8, four mice; and day 9, two mice. (C) Percentage of virus-induced CD8$^+$ T cells in the spleen. Mice were infected i.v. with 10^5 IU of LCMV. On days 8 and 9, single-cell suspensions were prepared from the spleens of three and two mice, respectively. The percentage of CD8$^+$ T cells within the mononuclear spleen cells was determined by flow cytometry following staining of the cells with phycoerythrin-labeled CD8-specific MAb. (D) The percentage of virus-specific CD8$^+$ T cells was measured by flow cytometry using MHC tetramers loaded with either of three H-2^b-restricted immunodominant epitopes of the LCMV, as described in Materials and Methods. The cumulative percentage for all three immunodominant epitopes is shown for individual mice. (E) Course of the LCMV-induced delayed type hypersensitivity footpad swelling reaction. Mice were infected by subcutaneous injection of 10^5 IU into the right hind footpads. From day 5 after infection, the dorsoventral thickness of the infected and the control feet was measured with spring-loaded calipers. The footpad swelling is expressed as the factor by which the thickness of the inoculated foot exceeded that of the noninoculated foot. The data represent the mean and standard error of four mice per group.

daily for survival. The WE strain of lymphocytic choriomeningitis virus (LCMV) was produced in L929 cells. Mice were infected with 10^5 IU in 0.3 ml PBS i.v. or by injection of 10^5 IU subcutaneously in 0.05 ml into the hind footpad. For determination of the virus titer in the spleen, weighed portions of the organ were homogenized in PBS and the number of PFU was determined with L929 cells. Levels of IFN-γ in the sera of mice were measured by a specific enzyme-linked immunosorbent assay according to the recommendations of the manufacturer (R&D Systems). The LCMV-induced delayed-type hypersensitivity (DTH) reaction was monitored by measuring the dorsoventral thickness of the inoculated and the contralateral hind footpads with spring-loaded calipers (Kroeplin). The swelling factor was calculated by dividing the thickness of the inoculated foot by that of the control foot.

Activation of IFN-inducible genes and Northern blot analysis. Bone marrow macrophages were plated at 10^6 in 6-cm dishes treated with medium, recombinant IFN-γ (1,000 U/ml) or IFN-α/β (1,000 U/ml) (Sigma). MEFs were treated with recombinant IFN-β (100 U/ml) (Calbiochem). After stimulation, cells were lysed and RNA was isolated with TRI-Reagent (Sigma) according to the manufacturer's protocol. RNA (5 to 10 μg/lane) was separated on 1% formaldehyde-agarose gels and blotted to a positively charged nylon membrane. Probes were radioactively labeled with Rediprime (Amersham) and hybridized with Express-Hyb-Solution (Clontech) according to the manufacturer's protocol.

RESULTS AND DISCUSSION

Lack of ISG15 does not affect embryogenesis, viability, or fertility. Mice lacking ISG15 were generated by replacing the complete coding region with a neomycin resistance cassette flanked by *loxP* sites by homologous recombination in ES cells (Fig. 1A). The desired mutation was identified by Southern blot analysis (Fig. 1B) and confirmed by Northern blotting (Fig. 1C). Western blot analysis of BMM before and after the induction of ISG15 with LPS and IFN-β was performed to demonstrate the absence of ISG15 protein and ISG15 conjugates (Fig. 1D and E). Thus, the established mouse strain, referred here as $ISG15^{-/-}$, is an ISG15 null mutant.

Intercrosses of $ISG15^{+/-}$ animals yielded homozygous, $ISG15^{-/-}$ mice in expected Mendel's ratios, indicating that embryogenesis was not negatively affected by the absence of ISG15. The mice lacking the ISG15 gene were viable, and their overall appearance was indistinguishable from $ISG15^{+/+}$ and $ISG15^{+/-}$ littermates inspected over >1 year.

The observation that ISG15 is up-regulated after conception in the uteri of mice, as well as of several other species, together with the notion on the inducible expression of ISG15 in bovine endometrium by IFN-τ, raised speculations about the role of ISG15 during implantation and pregnancy (2). However, the mating of homozygous, $ISG15^{-/-}$ mice yielded the same number of littermates as $ISG15^{+/+}$ mice (data not shown), which strongly argues against an essential and nonredundant role of ISG15 in murine fertility or pregnancy.

Loss of ISG15 does not affect the development and distribution of the major cell lineages of the immune system. It was reported that ISG15 is secreted from monocytes, lymphocytes, and nonimmune cells upon induction by different factors, including IFN-α and IFN-β, and was proposed to function as a cytokine (5). To determine whether ISG15 plays a role in establishing the major cell populations of the immune system, the thymus, bone marrow, spleen, and lymph nodes were analyzed by flow cytometry. As documented in Table 1, no significant differences between $ISG15^{+/+}$ and $ISG15^{-/-}$ mice in frequencies of analyzed cell populations were detected. Thus, the lack of ISG15 does not affect the composition of the main cellular compartments of the immune system in a steady-state situation. In addition, major cell populations of spleen and thymus were analyzed after induction of ISG15 by daily injections with poly(I:C) for 3 days. As shown in Table 2 no significant difference could be detected under these conditions between wild-type and $ISG15^{-/-}$ animals.

Lack of ISG 15 does not affect poly(I:C)-induced NK cell proliferation and NK cell activity. Immunoregulatory properties of ISG15 in its secreted form (4) had been postulated based on in vitro experiments performed with recombinant human ISG15 on B cell-depleted lymphocytes. In these investigations, ISG15 induced the production of IFN-γ, the proliferation of $CD56^+$ NK cells, and the formation of LAK cells. To address whether the proliferation of NK cells is affected by the loss of ISG15, $ISG15^{+/+}$ and $ISG15^{-/-}$ mice were stimulated with poly(I:C) for 36 h or alternatively for 3 days with daily injections of poly(I:C), and frequencies of NK cells were determined. As seen in Table 3, the numbers of NK cells were comparable in both types of mice.

To investigate whether the ISG15 deletion affected the activity of NK cells, the ability to lyse NK-susceptible YAC-1 tumor cells was assessed. Neither unfractionated $ISG15^{-/-}$ splenocytes (Fig. 2A) nor $ISG15^{-/-}$ cells that had been highly enriched for NK cells by $DX5^+$ selection (Fig. 2B) displayed any defect in their cytolytic activity against YAC-1 target cells.

Furthermore, in vivo activity of NK cells was tested in an NK cell-dependent tumor rejection assay using RMA-S tumor cells that lack MHC-I (12, 33). In this assay, tumor incidence was not enhanced in the absence of ISG15 (data not shown).

Together, our results do not provide any evidence for a significant role of ISG15 in NK cell proliferation and function.

Unimpaired antiviral responses of $ISG15^{-/-}$ mice against VSV and LCMV. The extremely strong and rapid induction of ISG15 by either viral infection or treatment with interferon or poly(I:C) suggests a possible role of this molecule in establishing an antiviral state of cells and in the regulation of immune responses. Therefore, the capability of MEFs derived from $ISG15^{-/-}$ mice to acquire an antiviral state upon treatment with IFN was assessed. As shown in Fig. 3A, IFN-β treatment protected $ISG15^{-/-}$ cells against the cytopathic effect of VSV to the same extent as control cells.

The immune response of mice against VSV is critically dependent on IFN and on STAT1 signaling, because mice lacking either the IFN-α receptor or STAT1 were shown to be highly susceptible to this virus (6, 22, 24). To reveal a possible involvement of ISG15 in the control of VSV infection, $ISG15^{-/-}$ mice were infected with graded doses of this virus. Neither the kinetics of virus-induced death nor the survival rate differed between $ISG15^{-/-}$ and $ISG^{+/+}$ mice (Fig. 3B). Thus, ISG15 is not indispensable for the control of this virus infection.

Antiviral cell-mediated immune responses of $ISG15^{-/-}$ mice were studied in mice acutely infected with the LCMV. During this infection, almost any cell type of the innate and adaptive immune system is strongly activated, but $CD8^+$ T cells were necessary and sufficient for the acute elimination of this virus. Since recombinant ISG15 has been reported to stimulate the secretion of IFN-γ by T cells prepared from the peripheral blood (4), the serum levels of IFN-γ during the early phase of LCMV infection were measured. As shown in Fig. 4A, identical titers of IFN-γ were detected in $ISG15^{-/-}$ and $ISG^{+/+}$ mice over the whole course of infection. Furthermore, the elimination of the LCMV from spleens did not

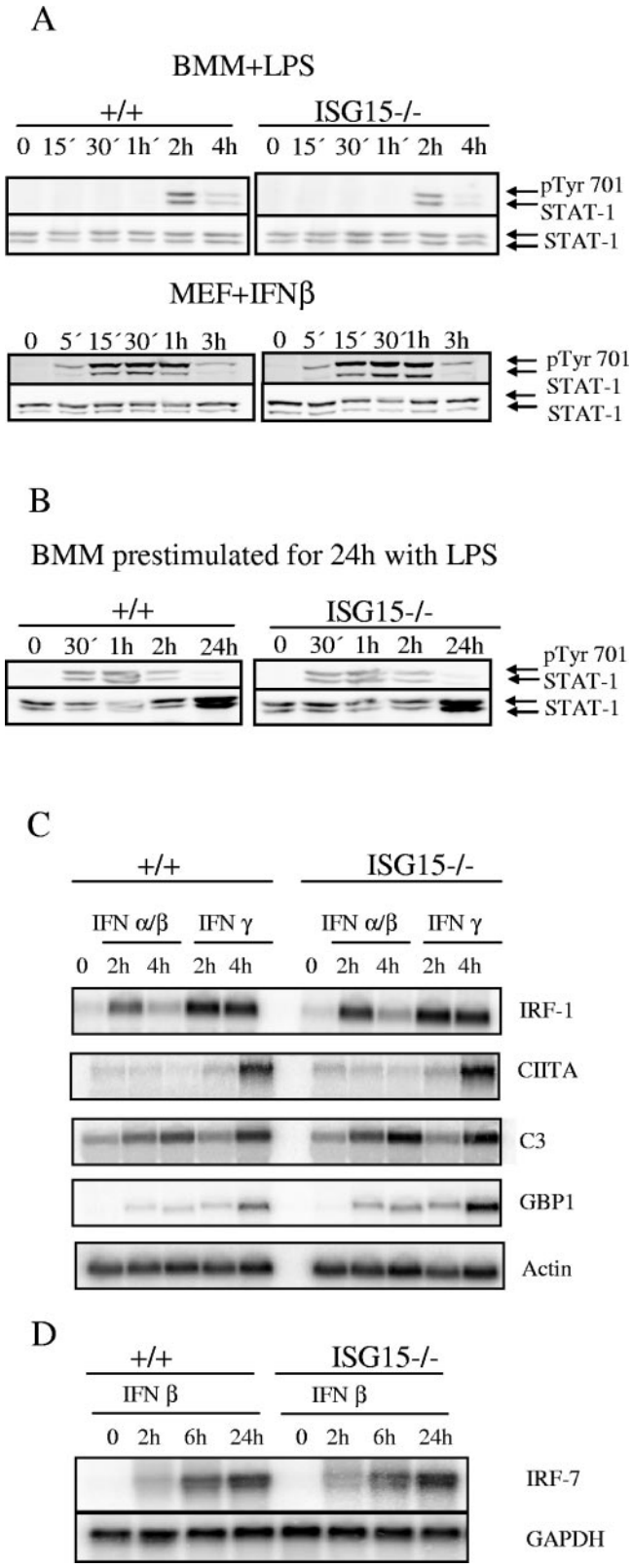

FIG. 5. STAT1 responses of ISG15$^{-/-}$ and ISG15$^{+/+}$ mice. (A) Bone marrow-derived macrophages and embryonic fibroblasts were stimulated with 100 ng/ml LPS and 100 U IFN-β, respectively. Western blots were incubated with anti-pTyr701 antibody to detect STAT1 phosphorylation. (B) Bone marrow-derived macrophages were prestimulated with 100 ng/ml LPS for 24 h. Cells were washed and stimulated 3 h later with 100 U/ml IFN-β for the times indicated. Western blots were incubated with anti-pTyr701 antibody to detect STAT1 phosphorylation (C) Bone marrow macrophages derived from ISG15$^{-/-}$ and ISG15$^{+/+}$ mice were stimulated with IFN-α/β or IFN-γ for the times indicated. Upon RNA isolation, Northern blots were hybridized with probes specific for the STAT1 target genes IRF-1, class II transactivator (CIITA), complement component c3 (C3), guanylate-binding protein-1 (GBP1) and β-actin as loading control. (D) Primary embryonic fibroblasts were stimulated with recombinant murine IFN-β for the times indicated. A Northern blot was hybridized with a probe specific for IRF-7 and upon stripping with a β-actin probe as a loading control.

significantly differ in either type of mice (Fig. 4B). Neither the expansion of splenic CD8$^+$ T cells in general (Fig. 4C) nor the percentage of CD8$^+$ cells specific for the three major immunodominant epitopes of the LCMV (Fig. 4D) differed significantly between ISG15$^{-/-}$ and wild-type controls. Finally, the DTH reaction induced by intraplantar injection of the virus into the hind footpad of mice was assessed. This DTH response is a biphasic swelling reaction mediated by CD8$^+$ or CD4$^+$ T cells in its first or second phase, respectively (23). As shown in Fig. 4E, neither the kinetics nor the intensity of the swelling reaction in ISG15$^{-/-}$ mice differed significantly from responses in wild-type controls. Thus, the lack of ISG15 did not significantly alter the activity of LCMV-induced NK cells or CD8$^+$ or CD4$^+$ T cells, indicating that ISG15 is not required for the proper activation or effector functions of these cells during LCMV infection.

Lack of ISG15 does not affect STAT1 (Y701) phosphorylation and the induction of typical STAT1 target genes. Malakhov et al. reported that STAT1 can be modified by the conjugation of ISG15 (18). Mice lacking UBP43, the deconjugating enzyme for ISG15, show prolonged STAT1 phosphorylation and enhanced expression of STAT1 target genes. These authors concluded that ISG15 conjugation is an important regulatory mechanism of JAK/STAT signaling and thus of interferon signal transduction (20, 28). We therefore analyzed STAT1 signaling in the absence of ISG15.

Macrophages and embryonic fibroblasts derived from ISG15$^{+/+}$ and ISG15$^{-/-}$ animals were stimulated with LPS and IFN-α/β, respectively, and the phosphorylation of STAT1 tyrosine 701 was examined. Neither in macrophages nor in MEFs was a difference detected in the kinetics of STAT1 phosphorylation between ISG15$^{+/+}$ and ISG15$^{-/-}$ cells (Fig. 5A). To test STAT1 phosphorylation in and ISG15$^{-/-}$ cells under high levels of ISG15 expression and ISG15 conjugation, BMM were prestimulated with LPS for 24 h to induce ISG15 and ISG15 conjugation. Subsequently, the cells were restimulated with IFN-β. Also under these conditions, no difference in the STAT1 phosphorylation was observed. Congruently, mRNA expression levels of typical STAT1 target genes—the IRF-1, class II transactivator (CIITA), complement component c3 (C3), guanylate-binding protein-1 (GBP1), and IRF7 genes—remained unchanged in the absence of ISG15 (Fig. 5C and D). Taken together, no evidence was found for an essential role of ISG15 in STAT1 signaling.

As STAT1 is indispensable for NK cell activity (12), these results are also in accord with the lack of any diminished activity of NK cells in the absence of ISG15.

Concluding remarks. Previously, a broad spectrum of biological activities were attributed directly to ISG15 and to protein modification by conjugation of ISG15. Given the fact that the main components of the ISG15 conjugation system (ISG15, UBE1L, UbcH8, and UBP43) are all induced by IFN, it is surprising that ISG15$^{-/-}$ mice did not reveal any failure in antiviral immune defense against VSV and LCMV or STAT1 signaling. Our results do not support the interpretation of data obtained with UBP43$^{-/-}$ mice that suggested an important role of ISG15 in the regulation of the JAK/STAT pathway and interferon signaling (20, 28). STAT1 modification and the functional alterations observed with UBP43$^{-/-}$ mice might result from the aberrantly enhanced ISG15 expression, together with defective deconjugation, and do not necessarily play a role under physiological conditions. Alternatively, UBP43 may have ISG15-independent activities.

Furthermore, we did not find any in vivo evidence to support the previous claims on cytokine-like activity of ISG15 (5) or its role during pregnancy (1).

Thus far, analysis of ISG15$^{-/-}$mice did not provide any evidence for a specific function that could be attributed to ISG15. Alternatively, ISG15 activity may be redundant, and its lack may be well compensated. However, due to the diversity of IFN and immune responses, it is also possible that challenging ISG15$^{-/-}$ mice with other pathogens or investigating them in other experimental settings might uncover specific functions for ISG15 and ISG15 conjugation. Identification of novel ISG15 target proteins could enlighten other as-yet-unknown activities of this protein modifier, and ISG15$^{-/-}$ mice will be an important tool to unravel their biological significance.

ACKNOWLEDGMENTS

This research was supported by Deutsche Forschungsgemeinschaft grants Ho 493/12 and KN 590/1.

We thank Marcus Wietstruk for excellent technical assistance and Elvira Rhode for blastocysts injection. We appreciate critical review of the manuscript by Robert Krug, Debbie Lenschowd, and Skip Virgin.

We declare that we have no competing financial interests.

REFERENCES

1. **Austin, K. J., B. M. Bany, E. L. Belden, L. A. Rempel, J. C. Cross, and T. R. Hansen.** 2003. Interferon-stimulated gene-15 (Isg15) expression is up-regulated in the mouse uterus in response to the implanting conceptus. Endocrinology **144:**3107–3113.
2. **Austin, K. J., A. L. Carr, J. K. Pru, C. E. Hearne, E. L. George, E. L. Belden, and T. R. Hansen.** 2004. Localization of ISG15 and conjugated proteins in bovine endometrium using immunohistochemistry and electron microscopy. Endocrinology **145:**967–975.
3. **Boehm, U., T. Klamp, M. Groot, and J. C. Howard.** 1997. Cellular responses to interferon-gamma. Annu. Rev. Immunol. **15:**749–795.
4. **D'Cunha, J., E. Knight, Jr., A. L. Haas, R. L. Truitt, and E. C. Borden.** 1996. Immunoregulatory properties of ISG15, an interferon-induced cytokine. Proc. Natl. Acad. Sci. USA **93:**211–215.
5. **D'Cunha, J., S. Ramanujam, R. J. Wagner, P. L. Witt, E. Knight, Jr., and E. C. Borden.** 1996. In vitro and in vivo secretion of human ISG15, an IFN-induced immunomodulatory cytokine. J. Immunol. **157:**4100–4108.
6. **Durbin, J. E., R. Hackenmiller, M. C. Simon, and D. E. Levy.** 1996. Targeted disruption of the mouse Stat1 gene results in compromised innate immunity to viral disease. Cell **84:**443–450.
7. **Haas, A. L., P. Ahrens, P. M. Bright, and H. Ankel.** 1987. Interferon induces a 15-kilodalton protein exhibiting marked homology to ubiquitin. J. Biol. Chem. **262:**11315–11323.
8. **Hamerman, J. A., F. Hayashi, L. A. Schroeder, S. P. Gygi, A. L. Haas, L. Hampson, P. Coughlin, R. Aebersold, and A. Aderem.** 2002. Serpin 2a is induced in activated macrophages and conjugates to a ubiquitin homolog. J. Immunol. **168:**2415–2423.
9. **Ihle, J. N.** 2001. The Stat family in cytokine signaling. Curr. Opin. Cell Biol. **13:**211–217.
10. **Knobeloch, K. P., M. D. Wright, A. F. Ochsenbein, O. Liesenfeld, J. Lohler, R. M. Zinkernagel, I. Horak, and Z. Orinska.** 2000. Targeted inactivation of the tetraspanin CD37 impairs T-cell-dependent B-cell response under suboptimal costimulatory conditions. Mol. Cell. Biol. **20:**5363–5369.
11. **Korant, B. D., D. C. Blomstrom, G. J. Jonak, and E. Knight, Jr.** 1984. Interferon-induced proteins. Purification and characterization of a 15,000-dalton protein from human and bovine cells induced by interferon. J. Biol. Chem. **259:**14835–14839.
12. **Lee, C. K., D. T. Rao, R. Gertner, R. Gimeno, A. B. Frey, and D. E. Levy.** 2000. Distinct requirements for IFNs and STAT1 in NK cell function. J. Immunol. **165:**3571–3577.
13. **Lefrancois, L.** 1984. Protection against lethal viral infection by neutralizing and nonneutralizing monoclonal antibodies: distinct mechanisms of action in vivo. J. Virol. **51:**208–214.
14. **Leinikki, P. O., J. Calderon, M. H. Luquette, and R. D. Schreiber.** 1987. Reduced receptor binding by a human interferon-gamma fragment lacking 11 carboxyl-terminal amino acids. J. Immunol. **139:**3360–3366.
15. **Levy, D. E. and J. E. Darnell, Jr.** 2002. Stats: transcriptional control and biological impact. Nat. Rev. Mol. Cell Biol. **3:**651–662.
16. **Li, J., G. W. Peet, D. Balzarano, X. Li, P. Massa, R. W. Barton, and K. B. Marcu.** 2001. Novel NEMO/IκB kinase and NF-κB target genes at the pre-B to immature B cell transition. J. Biol. Chem. **276:**18579–18590.
17. **Loeb, K. R., and A. L. Haas.** 1992. The interferon-inducible 15-kDa ubiquitin homolog conjugates to intracellular proteins. J. Biol. Chem. **267:**7806–7813.
18. **Malakhov, M. P., K. I. Kim, O. A. Malakhova, B. S. Jacobs, E. C. Borden, and D. E. Zhang.** 2003. High-throughput immunoblotting. Ubiquitin-like protein ISG15 modifies key regulators of signal transduction. J. Biol. Chem. **278:**16608–16613.
19. **Malakhov, M. P., O. A. Malakhova, K. I. Kim, K. J. Ritchie, and D. E. Zhang.** 2002. UBP43 (USP18) specifically removes ISG15 from conjugated proteins. J. Biol. Chem. **277:**9976–9981.
20. **Malakhova, O. A., M. Yan, M. P. Malakhov, Y. Yuan, K. J. Ritchie, K. I. Kim, L. F. Peterson, K. Shuai, and D. E. Zhang.** 2003. Protein ISGylation modulates the JAK-STAT signaling pathway. Genes Dev. **17:**455–460.
21. **Manthey, C. L., S. W. Wang, S. D. Kinney, and Z. Yao.** 1998. SB202190, a selective inhibitor of p38 mitogen-activated protein kinase, is a powerful regulator of LPS-induced mRNAs in monocytes. J. Leukoc. Biol. **64:**409–417.
22. **Meraz, M. A., J. M. White, K. C. Sheehan, E. A. Bach, S. J. Rodig, A. S. Dighe, D. H. Kaplan, J. K. Riley, A. C. Greenlund, D. Campbell, K. Carver-Moore, R. N. DuBois, R. Clark, M. Aguet, and R. D. Schreiber.** 1996. Targeted disruption of the Stat1 gene in mice reveals unexpected physiologic specificity in the JAK-STAT signaling pathway. Cell **84:**431–442.
23. **Moskophidis, D., and F. Lehmann-Grube.** 1989. Virus-induced delayed-type hypersensitivity reaction is sequentially mediated by CD8+ and CD4+ T lymphocytes. Proc. Natl. Acad. Sci. USA **86:**3291–3295.
24. **Muller, U., U. Steinhoff, L. F. Reis, S. Hemmi, J. Pavlovic, R. M. Zinkernagel, and M. Aguet.** 1994. Functional role of type I and type II interferons in antiviral defense. Science **264:**1918–1921.
25. **O'Shea, J. J., M. Gadina, and R. D. Schreiber.** 2002. Cytokine signaling in 2002: new surprises in the Jak/Stat pathway. Cell **109**(Suppl.)**:**S121–S131.
26. **Potter, J. L., J. Narasimhan, L. Mende-Mueller, and A. L. Haas.** 1999. Precursor processing of pro-ISG15/UCRP, an interferon-beta-induced ubiquitin-like protein. J. Biol. Chem. **274:**25061–25068.
27. **Ritchie, K. J., M. P. Malakhov, C. J. Hetherington, L. Zhou, M. T. Little, O. A. Malakhova, J. C. Sipe, S. H. Orkin, and D. E. Zhang.** 2002. Dysregulation of protein modification by ISG15 results in brain cell injury. Genes Dev. **16:**2207–2212.
28. **Ritchie, K. J., and D. E. Zhang.** 2004. ISG15: the immunological kin of ubiquitin. Semin. Cell Dev. Biol. **15:**237–246.
29. **Rosenbauer, F., A. Kallies, M. Scheller, K. P. Knobeloch, C. O. Rock, M. Schwieger, C. Stocking, and I. Horak.** 2002. Disabled-2 is transcriptionally regulated by ICSBP and augments macrophage spreading and adhesion. EMBO J. **21:**211–220.
30. **Schwartz, D. C., and M. Hochstrasser.** 2003. A superfamily of protein tags: ubiquitin, SUMO and related modifiers. Trends Biochem. Sci. **28:**321–328.
31. **Shackelford, J., and J. S. Pagano.** 2004. Tumor viruses and cell signaling pathways: deubiquitination versus ubiquitination. Mol. Cell. Biol. **24:**5089–5093.
32. **Stark, G. R., I. M. Kerr, B. R. Williams, R. H. Silverman, and R. D. Schreiber.** 1998. How cells respond to interferons. Annu. Rev. Biochem. **67:**227–264.
33. **van den Broek, M. F., D. Kagi, R. M. Zinkernagel, and H. Hengartner.** 1995. Perforin dependence of natural killer cell-mediated tumor control in vivo. Eur. J. Immunol. **25:**3514–3516.
34. **Yuan, W., and R. M. Krug.** 2001. Influenza B virus NS1 protein inhibits conjugation of the interferon (IFN)-induced ubiquitin-like ISG15 protein. EMBO J. **20:**362–371.
35. **Zhao, C., S. L. Beaudenon, M. L. Kelley, M. B. Waddell, W. Yuan, B. A. Schulman, J. M. Huibregtse, and R. M. Krug.** 2004. The UbcH8 ubiquitin E2 enzyme is also the E2 enzyme for ISG15, an IFN-alpha/beta-induced ubiquitin-like protein. Proc. Natl. Acad. Sci. USA **101:**7578–7582.